International Journal of Modern Physics C

EFFECTS OF LANGMUIR KINETICS ON TWO-LANE TOTALLY ASYMMETRIC EXCLUSION PROCESSES OF MOLECULAR MOTOR TRAFFIC

RUILI WANG*
Institute of Information Sciences and Technology, Massey University, New Zealand
r.wang@massey.ac.nz

RUI JIANG
School of Engineering Science, University of Science and Technology of China, Hefei, China
rjiang@ustc.edu.cn

MINGZHE LIU
Institute of Information Sciences and Technology, Massey University, New Zealand
m.z.liu@massey.ac.nz

JIMING LIU
School of Computer Science, University of Windsor, Windsor, Ontario, Canada
jiming@uwindsor.ca

QING-SONG WU
School of Engineering Science, University of Science and Technology of China, Hefei, China
qswu@ustc.edu.cn

Received Day Month Year
Revised Day Month Year

In this paper, we study a two-lane totally asymmetric simple exclusion process (TASEP) coupled with random attachment and detachment of particles (Langmuir kinetics) in both lanes under open boundary conditions. Our model can describe the directed motion of molecular motors, attachment and detachment of motors, and free inter-lane transition of motors between filaments. In this paper, we focus on some finite-size effects of the system because normally the sizes of most real systems are finite and small (e.g., size $\leq 10,000$). A special finite-size effect of the two-lane system has been observed, which is that the density wall moves left first and then move towards the right with the increase of the lane-changing rate. We called it the jumping effect. We find that increasing attachment and detachment rates will weaken the jumping effect. We also confirmed that when the size of the two-lane system is large enough, the jumping effect disappears, and the two-lane system has a similar density profile to a single-lane TASEP coupled with Langmuir kinetics. Increasing lane-changing rates has little effect on density profiles after the density reaches maximum. Also, lane-changing rate has no effect on density profiles

*Corresponding author.

of a two-lane TASEP coupled with Langmuir kinetics at a large attachment/detachment rate and/or a large system size. Mean-field approximation is presented and it agrees with our Monte Carlo simulations.

Keywords: Langmuir kinetics; two-lane TASEPs; density profiles; jumping effects.

1. Introduction

Recently, driven diffusive systems have attracted the interests of physicists because the systems show surprisingly rich and complex behavior.[1,2,3,4,5,6] As a simple model of driven diffusive systems, asymmetric simple exclusion processes (ASEPs) have been widely studied in chemistry and physics.[7,8] Moreover, ASEPs have been applied successfully in biology such as gel electrophoresis,[9] protein synthesis,[10,11] mRNA translation phenomena,[12] motion of molecular motors along the cytoskeletal filaments,[13,14] and the depolymerization of microtubules by special enzymes[15] as well as vehicular traffic.[16]

A totally asymmetric simple exclusion process (TASEP) is regarded as the minimal model of ASEPs, in which particles move along one direction. TASEP has received much attention in modeling intra-cellular molecular transport and related traffic problems[15,17,18,19,20,21,22] in recent years.

MacDonald et al.[17] initially used an TASEP to simulate the dynamics of ribosomes moving along messenger RNA chains. Kruse and Sekimoto[18] proposed a two-headed TASEP model to describe molecular motor traffic. In their model, each motor consists of two heads and each head is attached to a filament. Each filament is assumed to be moveable. The investigation indicates that the average relative velocity of filaments is a non-monotonic function of the concentration of motors. The density and current profiles of motors with different types of microtubule tracks (e.g., cylindrical geometry and radial geometry) have been investigated by Lipowsky et al.[19]

An extension of single-lane TASEPs, incorporating Langmuir kinetics (LK, the attachment and detachment of particles), has been presented by Parmeggiani et al.[20] Their model is also referred to as the PFF model. Numerical results of the PFF model show that there are unexpected stationary regimes for large but finite systems. Such regimes are represented by phase coexistence in both low and high density regions, which are separated by a domain wall.

A model, incorporating a single-lane TASEP, Langmuir kinetics and Brownian ratchet mechanism,[23] is proposed by Nishinari et al.[21] to mimic the movement of the single-headed kinesin motor, KIF1A. A novel feature in their model is that there are *three* states (strong binding, weak binding and no binding) of a KIF1A, compared to *two* states (binding or unbinding) in previous models. Their model can capture explicitly the effects of adenosine triphosphate (ATP) hydrolysis as well as the ratchet mechanism which drives individual motors. The experimentally observed single molecular properties in the low-density limit are reproduced and a phase diagram is presented.

Most previous work on modeling molecular motor traffic deals with single-lane systems where particles can move forward or backward, or attach and detach to a bulk (a collection of sites in a lane except boundaries). Obviously, the description of the traffic of motors would be more realistic if multi-lane asymmetric exclusion processes can be considered. Experimental observations[24] have found that motor protein kinesins can move along parallel protofilaments of microtubules and they can jump between these protofilaments without restraint.

Recently, Pronina and Kolomeisky[25] proposed a two-lane traffic model to simulate a two-lane TASEP with symmetric lane-changing rules between two lanes, but without Langmuir kinetics. The computational results suggest that lane-changing rates have a strong effect on the steady-state properties of the system. In particular, the particle current of each lane will decrease and particle densities will increase with the increase of particle coupling. Pronina and Kolomeisky then extended their model to a more general case where asymmetric coupling is applied.[26] It is found that asymmetric coupling between lanes leads to a very complex phase diagram, quite different from symmetric coupling. There are seven phases in the TASEP with asymmetric lane-changing rates, in contrast to three phases found in the system with symmetric coupling. In addition, a new maximal-current phase with a domain wall in the intermediate coupling is reported in Ref.[26].

Effects of synchronization of kinks (i.e., domain walls) in a two-lane TASEP without Langmuir kinetics is investigated by Mitsudo and Hayakawa.[27] The asymmetric lane-changing rate between lanes is used. Moreover, different injection and ejection rates of particles at the boundaries of two lanes are also considered. The positions of kinks are reported to be synchronized, though the number of particles may be different on these two lanes. Reichenbach *et al.* [28] proposed a generic transportation model by introducing internal states into driven exclusion processes. The internal states provide a unique way to describe the flow of particles.

More recently, Jiang et al.[29] introduced Langmuir kinetics into one lane of a two-lane system. This has shown that synchronization of shocks on both lanes occurs when the lane-changing rate exceeds a threshold. A boundary layer is also observed at the left boundary as a finite-size effect. In their model, attachment and detachment of particles are assumed to occur only on one of two lanes, not both, which is unable to realistically describe real two-lane or multi-lane molecular motor traffic.

This paper will investigate the collective effect of attaching and detaching particles on both lanes of a two-lane system with symmetric inter-lane coupling. In particular, we will focus on the finite-size effects of the system. The model described in this paper is directly motivated by the dynamics of molecular motors, for instance, unidirectional motion of molecular motors along filaments,[30] random motor (e.g., kinesin) attachments and detachments to filaments,[31] and molecular motors freely changing to adjacent filaments.[24] It is expected that the incorporated process of a two-lane TASEP, Langmuir kinetics and lane-changing can shed light on the study of the traffic of molecular motors and other particle traffic in biology.

We investigate the effects of the following parameters on density and current profiles: (i) Different lane-changing rates ω. We denote $\Omega = \omega N$, where Ω is used to represent the number of lane-changing particles and N is the length of each lane (i.e., the number of cells in each lane); (ii) Different combinations of attachment ($\Omega_A = \omega_A N$) and detachment ($\Omega_D = \omega_D N$) rates (for simplicity, we assume that attachment rate Ω_A is fixed but detachment rate Ω_D varies); and (iii) Different system size N, i.e., the length of each lane. Note that as we only consider symmetric lane changing, these two lanes are equivalent. We compare results obtained from our model when $\Omega > 0$ and $\Omega = 0$ (where the two-lane system becomes two separated TASEPs coupled with Langmuir kinetics). In this way, we can more clearly distinguish the effect of different values of Ω on a two-lane system. Finally, mean-field approximation (MFA) is presented and used to verify our Monte Carlo simulations (MCS).

The paper is organized as follows. In Section II, we give a description of our two-lane TASEP model, considering attachment and detachment of particles in both lanes. In Section III, we present and discuss the results of our Monte Carlo simulations. In Section IV, mean-field approximation is presented and the quantitative agreement between the Monte Carlo simulations and the mean-field theory is confirmed. Finally, we give our conclusions in Section V.

2. Model

Our model is defined in a two-lane lattice of $N \times 2$ sites, where N is the length of a lane. We assume that all particles move from the left to the right, as shown in Fig. 1. Sites $i = 1$ and $i = N$ define the left and right boundaries respectively, while a set of sites $i = 2$, ..., $N - 1$ is referred to as a bulk. Particles in the system are involved in the following processes: lane selection, particle injection into the first site of a lane, particle detachment from a bulk, particle movement along a bulk, particle lane-changing between bulks, particle attachment to a bulk, and particle ejection from the last site of a lane. Thus, we assume that a particle that is injected to a lane and moves along the lane may be involved in the following processes:

- Lane selection: A lane is randomly chosen.
- Particle injection: If the first site of the selected lane is unoccupied, a particle will be injected to the site with probability α.
- Particle detachment: A particle can leave the system with probability ω_D.
- Particle movement: If a particle cannot leave the system, it can move forward to the next site in the same lane provided that the next site is empty. If the next site is not empty, the particle cannot advance. In this case, the particle will check if it can change to the other lane.
- Particle lane-changing: The particle may change to the corresponding site on the other lane with probability ω if the corresponding site on the other lane is unoccupied.
- Particle attachment: If a site in a bulk is empty, a particle can attach to

the site with probability ω_A.

- Particle ejection: If a particle reaches the last site of a lane, it will be ejected from the system with probability β.

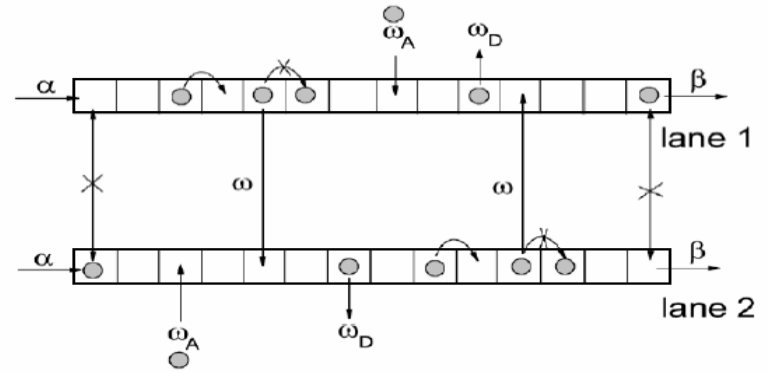

Fig. 1. The schematic representation of a two-lane TASEP with symmetric inter-lane coupling, and the attachment and detachment of particles on both lanes.

The above processes can be described using the following updating rules. As the two lanes are equivalent, they have the same updating rules. We only list the updating rules for lane 2. An occupation variable ($\tau_{\ell,i}$) denotes the state of the ith site in the ℓth lane, where $\tau_{\ell,i} = 1$ (or $\tau_{\ell,i} = 0$) corresponds to whether the site is occupied (or empty). Thus, $\tau_{2,i}$ refers to the state of site i on lane 2. The rules are:

- Case $i = 1$. (i) If $\tau_{2,1} = 0$, a particle enters the system with probability α; (ii) If $\tau_{2,1} = 1$ and $\tau_{2,2} = 0$, then the particle in site $(2, 1)$ moves into site $(2, 2)$; (iii) If $\tau_{2,1} = 1$ and $\tau_{2,2} = 1$, then the particle in site $(2, 1)$ stays there. No lane change occurs.[a]
- Case $i = N$. If $\tau_{2,N} = 1$, the particle leaves the system with probability β. No lane change occurs.[b]
- Case $1 < i < N$. (i) If $\tau_{2,i} = 1$, the particle may leave the system with probability ω_D; If it cannot leave the system, it moves into site $(2, i + 1)$ provided $\tau_{2,i+1} = 0$. If the particle cannot advance, it may change to lane 1 with probability ω if $\tau_{1,i} = 0$; (ii) If $\tau_{2,i} = 0$, a particle enters the system with probability ω_A.

These updating rules for both lanes are illustrated in Fig. 1. For simplicity, we use a symmetric lane-changing rule. It will be the next step of our work to investigate the

[a]The simulation results show that they are essentially the same if lane-changing is allowed on the first site.

[b]The simulation results also show that there are no differences on density profiles whether lane-changing is considered in the last site.

effects of asymmetric lane-changing rates on the dynamics of interacting particles.

Normally, there are three types of updating schemes:[32] (i) In parallel. Updating rules are synchronously applied to all sites. A typical application is in vehicular traffic flow; (ii) In ordered sequence. Positions of particles are updated in an ordered sequential manner, e.g., from one end to the other end of a one-dimensional system; (iii) In random. A site is randomly chosen and it is updated according to updating rules. Here we use a randomly sequential updating scheme, i.e., the third scheme, which has been widely used in the simulations of molecular motor traffic.[18,19,20,21,25,26,29]

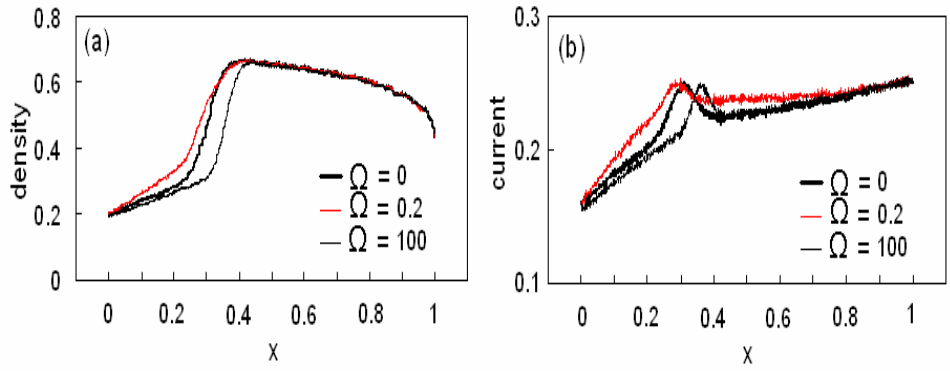

Fig. 2. (Color online) (a) Average density $\rho(x)$, and (b) Current $J(x)$ for different Ω. $\Omega = 0$ is the thick solid line in the middle ; $\Omega = 0.2$ is the red/light line on the left of the $\Omega = 0$ line; $\Omega = 100$ is the solid line on the right. $x = i/N$. The system parameters are set to: $N = 1000$, $\Omega_A = 0.3$, $\Omega_D = 0.1$, $\alpha = 0.2$ and $\beta = 0.6$.

3. Monte Carlo Simulations

In this section, the results of our Monte Carlo simulations are presented. As suggested in [20], in large system sizes ($N \gg 1$), the Langmuir kinetic rates decrease synchronously with the system sizes, that is, $\Omega_A = \omega_A N$, $\Omega_D = \omega_D N$ and the bonding constant $K = \Omega_A/\Omega_D$. Similarly, we define $\Omega = \omega N$. In simulations, stationary profiles are obtained by averaging 10^5 samples at each site. The sampling time interval is $10N$. The first $10^5 N$ time steps are discarded to let the transient time out. For the special case when $\Omega = 0$, the two-lane process is reduced to two separated processes: two one-lane TASEP with Langmuir kinetics. Features of a one-lane TASEP with Langmuir kinetics have been well studied in Ref.[20]

Fig. 2 shows average density $\rho(x)$ and current $J(x)$ of one lane of a two-lane system for different values of Ω, where $x = i/N$. For a special case $\Omega = 0$, the two-lane system reduces to two separated single-lane systems. When Ω increases, we may expect the domain wall always moves in one direction (either to the left or

right). However, an unexpected phenomenon has been observed in our simulations: the domain wall first moves to the left slightly, and then moves towards the right with the increase of Ω (see Fig. 2(a)). This process is more clearly captured in Figs. 3(a) and (b), where the domain walls for $\Omega \leq 0.4$ are shown. One can see that the domain wall moves to the left first when Ω increases from 0 to 0.2, and then moves towards the right when $\Omega > 0.2$. We refer to this feature as the *jumping effect* to describe the domain wall (as well as current curve) moving to the left and then to the right caused by particles jumping between the two lanes. We also find that there is a critical value, $\Omega_c \approx 0.2$, to distinguish the movement direction of the domain wall under certain conditions. A similar effect occurs in Ref.[29]

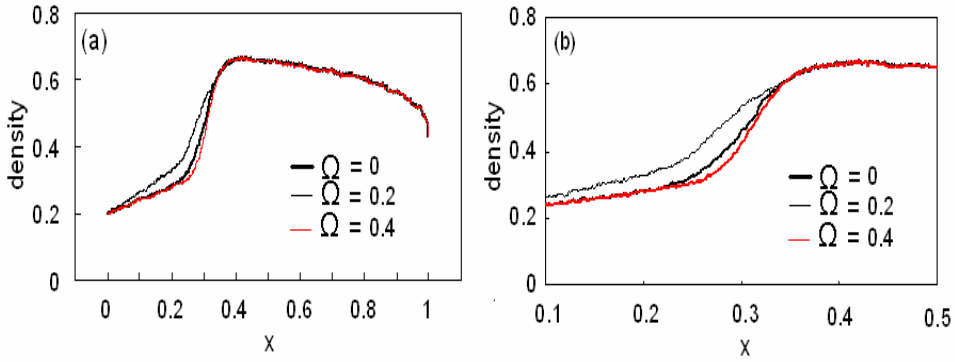

Fig. 3. (Color online) (a) Average density $\rho(x)$ for small values of Ω; (b) is a locally enlarged figure of (a). $\Omega = 0$ is the thick solid line in the middle; $\Omega = 0.2$ is the grey/light line on the left of the $\Omega = 0$ line ; $\Omega = 0.4$ is the red line on the right. $x = i/N$. The system parameters are: $N = 1000$, $\Omega_A = 0.3$, $\Omega_D = 0.1$, $\alpha = 0.2$ and $\beta = 0.6$.

When Ω_A and Ω_D increase proportionally, the jumping effect becomes weaker (comparing Fig. 2(a) with Figs. 4(a) and (b)). This implies that the jumping effect is also influenced by attachment and detachment rates.

The jumping effect is also observed in a larger system, e.g., $N = 10,000$, (see Fig. 5) when Ω is small. It can be seen that the domain wall moves left when $\Omega \leq 0.3$. When $\Omega > 0.3$, the domain wall moves right. For instance, there is an obvious movement towards right when $\Omega = 0.4$ (see Fig. 5(b)). The critical value Ω_c of Ω varies with a system size, i.e., Ω_c changes from 0.2 to 0.3 when the system size increases from 1,000 to 10,000.

We have also confirmed that the jumping effect in a two-lane homogeneous TASEP coupled with Langmuir kinetics is a kind of finite-size effect. When the system size is very large, e.g., $N = 100,000$, in our simulations, the jumping effect almost disappears.

We argue that we need to study and examine finite-size effects, like the jumping effect because the size of a real system is normally not very large. For example,

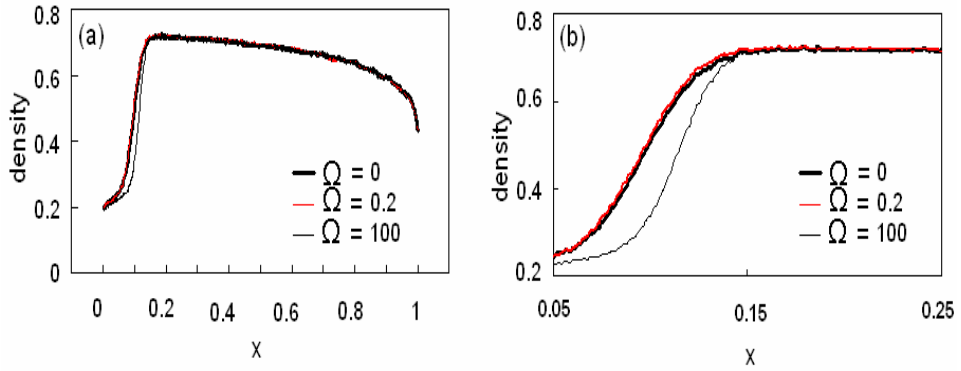

Fig. 4. (Color online) (a) Average density $\rho(x)$ for different Ω. (b) is a locally enlarged figure of (a). $\Omega = 0$ is the thick solid line in the middle; $\Omega = 0.2$ is the red line on the left and very close to the $\Omega = 0$ line ; $\Omega = 100$ is the line on the right. $x = i/N$. The system parameters are: $N = 1,000$, $\Omega_A = 0.6$, $\Omega_D = 0.2$, $\alpha = 0.2$ and $\beta = 0.6$.

kinesin protein motors are responsible for long-distance transport in a cell. The length that a kinesin protein motor travels from its origin to its destination is normally about 100 successive steps on microtubules and the step size of kinesins is about 8nm.[37] This indicates that a system size below 1,000 is enough to realistically describe the movements of molecular motors. Even for a large system, a size $N \leq 10,000$ is normally adequate for simulation. Thus, a conclusion obtained based on the assumption of an infinite size may not be applicable to any real system.

Comparing Fig. 2(a) with Figs. 4(a) and (b), it can be seen that the slopes of domain walls increase with the increase of Ω_A and Ω_D proportionally. This is because when the difference between Ω_A and Ω_D enlarges, more particles will attach to these two lanes rather than detach from them.

Increasing the value of Ω means more particles have chances to change to the other lane if they cannot move forward along the current lane. Upon further increasing Ω, it is found that the density decreases, and the locations of shocks shift right slightly (see Figs. 2(a) and 3(a)).

When $x > x_{max}^{den}$ (x_{max}^{den} denotes the position where the density reaches maximum), the differences between density profiles are not obvious (see Figs. 2 and 4). This suggests that lane-changing rate Ω does not have any obvious effect on the system properties (e.g., average density and current profiles) after the maximum density is reached.

We next investigate the effect of the values of K on average density and current profiles. We consider the situation in which Ω_A is fixed but Ω_D varies. Note that the increase of K means the decrease of Ω_D. It can be seen that average density increases with the increase of the value of K (see Fig. 6(a)). Moreover, the shock moves left and the amplitude increases. In other words, the width of the transition region decreases. This can be explained as follows: when the value of K increases,

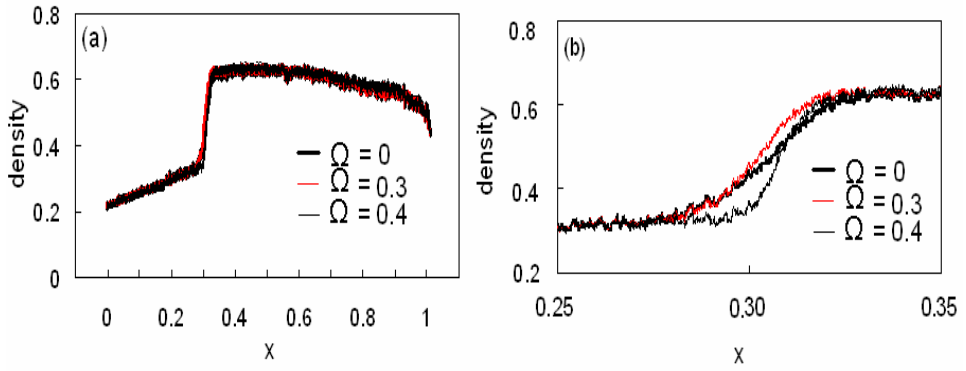

Fig. 5. (Color online) (a) Average density $\rho(x)$ for small values of Ω in a large system. (b) is a locally enlarged figure of (a). $\Omega = 0$ is the thick solid line in the middle, while $\Omega = 0.3$ is the red/light line slightly above it; $\Omega = 0.4$ is the solid line slightly below it. $x = i/N$. The system parameters are: $N = 10,000$, $\Omega_A = 0.3$, $\Omega_D = 0.1$, $\alpha = 0.2$ and $\beta = 0.6$.

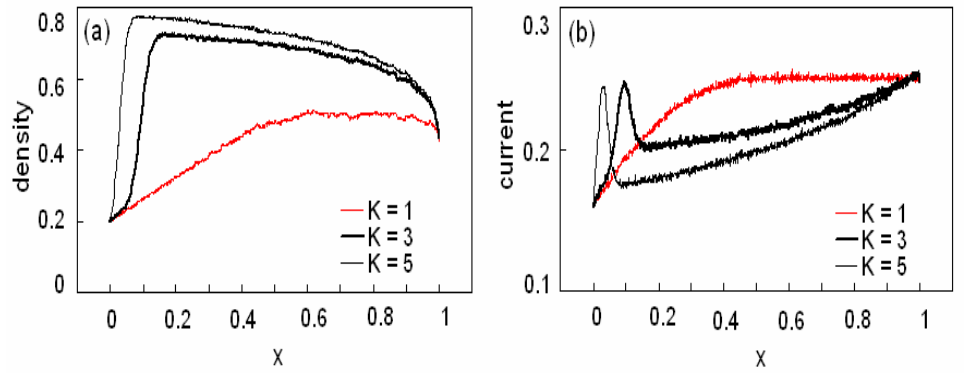

Fig. 6. (Color online) (a) Average density $\rho(x)$ for different values of K. (b) Current J(x) for different of K. In each figure, $K = 1$ is the shortest line; $K = 3$ is the line in the middle; $K = 5$ is the longest line. $x = i/N$. The system parameters are: $N = 1000$, $\Omega_A = 0.3$, $\Omega_D = 0.1$, $\alpha = 0.2$ and $\beta = 0.6$.

the value of Ω_D decreases proportionally, so that the opportunities for particles to detach from the bulk become smaller. In this case, more particles will remain in the bulk. This leads to an increase of average density.

In Fig. 6(b), the current first increases with the increase of the value of K till it reaches the maximum value, and then the current decreases with the increase of the value of K. In other words, the position with the maximum current moves left and the amplitude increases (see Fig. 6(b)) upon increasing K. The current curves can be obtained from equation $J_i \approx \rho_i(1 - \rho_{i+1})$, it thus can be seen that the maximum current $J_{max} \approx 0.25$ when densities of two adjacent sites are equal to 0.5. When

density is higher or lower than 0.5, the corresponding current is lower than 0.25.

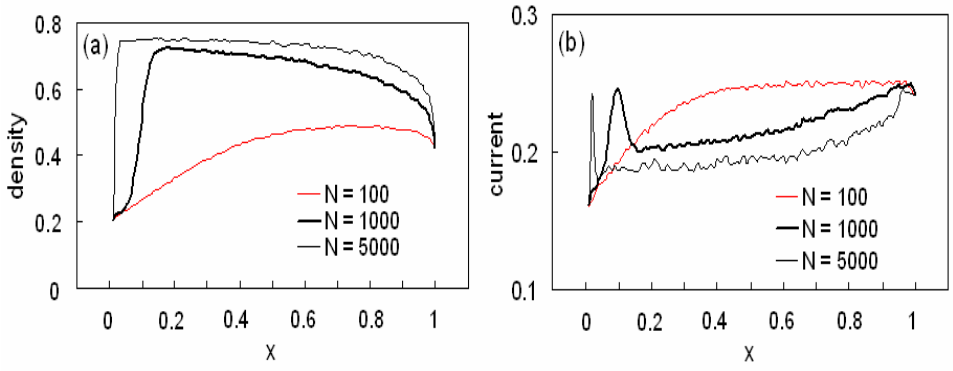

Fig. 7. (a) Average density $\rho(x)$; (b) Current $J(x)$ for different values of the system size N. In each figure, $N = 100$ is the shortest line in red; $N = 1000$ is the line in the middle; $N = 5000$ is the longest line. $x = i/N$. The system parameters are: $\Omega = 0.2$, $\Omega_A = 0.6$, $\Omega_D = 0.2$, $\alpha = 0.2$ and $\beta = 0.6$.

Fig. 7 shows the density and current profiles for different system sizes. It is found that the width of the transition region decreases as the number of sites is increased (see Fig. 7(a)). Our simulation suggests the boundary layer shows a finite-size effect and will disappear in the limit of an infinite system. The finite-size effect shown in Fig. 7(a) is consistent with that in Refs.[20,29] In Fig. 7(b) one observes the amplitude in the left boundary enhances when the system size increases.

4. Mean-field Approximation

In this section, a mean-field theory is developed. The occupation variable ($\tau_{\ell,i}$) defined in section II is also used. The corresponding equation for the evolution of particle densities $\langle\tau_{\ell,i}\rangle$ in a bulk (i.e., $1 < i < N$) can be written as

$$\begin{aligned}\frac{d\langle\tau_{1,i}\rangle}{dt} &= \langle\tau_{1,i-1}(1-\tau_{1,i})\rangle - \langle\tau_{1,i}(1-\tau_{1,i+1})\rangle \\ &+ \omega\langle\tau_{2,i}\tau_{2,i+1}(1-\tau_{1,i})\rangle - \omega\langle\tau_{1,i}\tau_{1,i+1}(1-\tau_{2,i})\rangle \\ &+\omega_A\langle 1-\tau_{1,i}\rangle - \omega_D\langle\tau_{1,i}\rangle, \end{aligned} \tag{1}$$

$$\begin{aligned}\frac{d\langle\tau_{2,i}\rangle}{dt} &= \langle\tau_{2,i-1}(1-\tau_{2,i})\rangle - \langle\tau_{2,i}(1-\tau_{2,i+1})\rangle \\ &+ \omega\langle\tau_{1,i}\tau_{1,i+1}(1-\tau_{2,i})\rangle - \omega\langle\tau_{2,i}\tau_{2,i+1}(1-\tau_{1,i})\rangle \\ &+\omega_A\langle 1-\tau_{2,i}\rangle - \omega_D\langle\tau_{2,i}\rangle, \end{aligned} \tag{2}$$

where $\langle\cdots\rangle$ denotes a statistical average. The term $\omega\langle\tau_{1,i}\tau_{1,i+1}(1-\tau_{2,i})\rangle$ is the average current from site i in lane 1 to site i in lane 2, while $\omega\langle\tau_{2,i}\tau_{2,i+1}(1-\tau_{1,i})\rangle$ is the average current from site i in lane 2 to site i in lane 1. The first two terms in Eqs. (1) and (2) correspond to particle movement; the middle two terms correspond to particle lane changing, and the last two terms correspond to attachment and detachment of particles. At the boundaries, the densities evolve as

$$\frac{d\langle\tau_{\ell,1}\rangle}{dt} = \alpha\langle 1-\tau_{\ell,1}\rangle - \langle\tau_{\ell,1}(1-\tau_{\ell,2})\rangle, \tag{3}$$

$$\frac{d\langle\tau_{\ell,N}\rangle}{dt} = \langle\tau_{\ell,N-1}(1-\tau_{\ell,N})\rangle - \beta\langle\tau_{\ell,N}\rangle, \tag{4}$$

where ℓ can be 1 or 2. It can be seen that Eqs. (1) and (2) are equivalent when we use the same lane-changing rate between two lanes. Therefore, we only focus on the mean-field approximation in lane 2 (i.e., Eq. (2)). When N is large, i.e., $N \gg 1$, we can transfer the coarse-grained stationary-state Eq. (2) to continuum mean-field approximation. First, we factorize correlation functions by replacing $\langle\tau_{\ell,i}\rangle$ and $\langle\tau_{\ell,i+1}\rangle$ with $\rho_{\ell,i}$ and $\rho_{\ell,i+1}$, then we set

$$\rho_{\ell,i\pm1} = \rho(x) \pm \frac{1}{N}\frac{\partial\rho}{\partial x} + \frac{1}{2N^2}\frac{\partial^2\rho}{\partial x^2} + O(\frac{1}{N^3}). \tag{5}$$

Substituting (5) into Eq. (2), we obtain

$$\begin{aligned}\frac{\partial\rho_2}{\partial t'} &= (2\rho_2-1)\frac{\partial\rho_2}{\partial x} + \Omega_A(1-\rho_2) - \Omega_D\rho_2 \\ &\quad -\Omega(1-\rho_1)\rho_2^2 + \Omega\rho_1^2(1-\rho_2),\end{aligned} \tag{6}$$

where $t' = t/N$, $\Omega = \omega N$, $\Omega_A = \omega_A N$ and $\Omega_D = \omega_D N$. The term $\langle\tau_{1,i}\tau_{1,i+1}(1-\tau_{2,i})\rangle$ is replaced by $\rho_{1,i}\rho_{1,i+1}(1-\rho_{2,i})$, and $\rho_{1,i+1}$ is approximated as $\rho_{1,i}$; similarly, the term $\langle\tau_{2,i}\tau_{2,i+1}(1-\tau_{1,i})\rangle$ is replaced by $\rho_{2,i}\rho_{2,i+1}(1-\rho_{1,i})$, and $\rho_{2,i+1}$ is approximated as $\rho_{2,i}$. The boundary conditions become $\rho_\ell(x=0) = \alpha$ and $\rho_\ell(x=1) = (1-\beta)$. As lane-changing is symmetric and two lanes are homogeneous, we have $\rho_2 = \rho_1 = \rho$ (our Monte Carlo simulations show that densities in lanes 1 and 2 are the same). Thus, Eq. (6) reduces to

$$\frac{\partial\rho}{\partial t'} = (2\rho-1)\frac{\partial\rho}{\partial x} + \Omega_A(1-\rho) - \Omega_D\rho. \tag{7}$$

In the limit of $t \to \infty$, the system reaches a stationary state with $\frac{\partial\rho}{\partial t'} = 0$, Eq. (7) simplifies into

$$(2\rho-1)\frac{\partial\rho}{\partial x} + \Omega_A(1-\rho) - \Omega_D\rho = 0. \tag{8}$$

Eq. (8) is a first order differential equation and has been solved in Ref.[35] The low-density profiles in the bulk can be obtained by integrating the equation from the left boundary ($\rho(0) = \alpha$) to a density ρ_l:

$$x = \frac{1}{\Omega_D(K+1)}[2(\rho_l-\alpha) + \frac{K-1}{K+1}\ln|\frac{K-(K+1)\rho_l}{K-(K+1)\alpha}|]. \tag{9}$$

Similarly, we can also integrate the equation from the right boundary ($\rho(1) = 1-\beta$) to a density ρ_r:

$$1 - x = \frac{1}{\Omega_D(K+1)}[2(1-\beta-\rho_r) + \frac{K-1}{K+1}\ln|\frac{K-(K+1)(1-\beta)}{K-(K+1)\rho_r}|], \qquad (10)$$

where $K = \Omega_A/\Omega_D$. The overall density profile across the system can be described by determining a shock position in these two profiles. In Fig. 8, we compare the results of mean-field approximation (MFA) with the results of Monte Carlo simulations (MCS). We find that the results of Monte Carlo simulations are in agreement with that of mean-field approximation. We note that numerical results of MCS in Figs. 8(a) and (b) are almost the same as Figs. 2 and 5 in Ref.,[35] which also suggests that lane-changing rate Ω has no effect on density profiles of a two-lane TASEP coupled with Langmuir kinetics at a large attachment/detachment rate and/or a large system size.

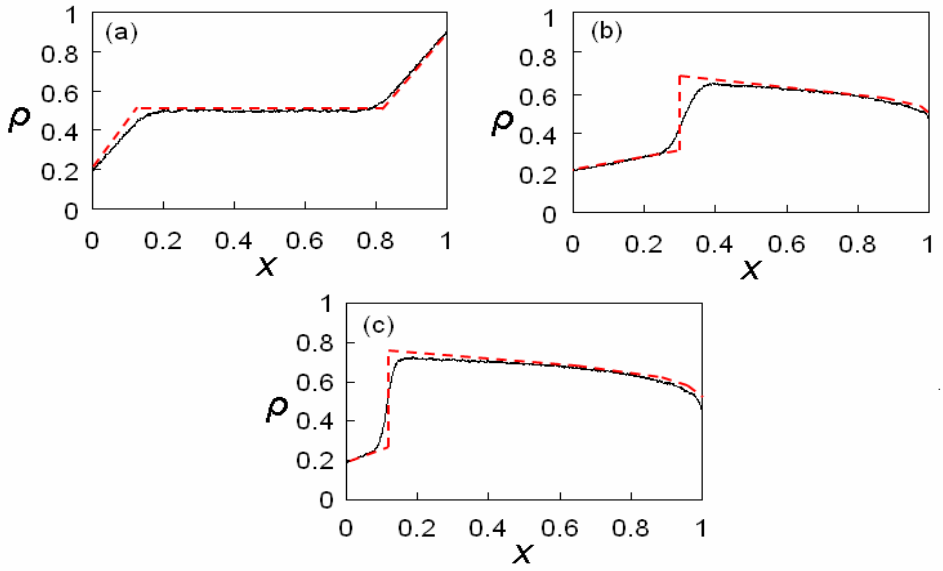

Fig. 8. (Color Online) Density profiles from Monte Carlo simulations (solid line) and mean-field approximation (red dashed line). (a) $\alpha = 0.2, \beta = 0.1, k = 1, \Omega_D = 0.1$ and $\Omega = 0.2$; (b) $\alpha = 0.2, \beta = 0.6, k = 3, \Omega_D = 0.1$ and $\Omega = 2$; (c) $\alpha = 0.2, \beta = 0.6, k = 3, \Omega_D = 0.2$ and $\Omega = 100$. The system size $N = 1,000$.

5. Conclusion

In this paper, two-lane totally asymmetric exclusion processes coupled with Langmuir kinetics on both lanes are studied using Monte Carlo simulations (MCS) and mean-field approximation (MFA). The results of Monte Carlo simulations agree

with the results of mean-field approximation. The model is directly inspired by the experimentally observed movement of molecular motors which include motor advancing along filaments, random attachment and detachment, and free jumping between filaments.

The system has mainly demonstrated the following complex behavior on two lanes.

- The *jumping* effect is observed, that is, the domain wall first moves left slightly, and then move towards the right with the increase of the lane-changing rate. This effect is a finite-size effect as it is not observed when the system is large, e.g., $N = 100,000$. On the other hand, increasing attachment and detachment rates proportionally will lead to the *jumping* effect becoming weaker (see Figs. 2 and 4).
- After densities reach maximum, the increase of the lane-changing rate has little effect on density profiles (see Figs. 2-5).
- When Ω_A (attachment rate) is fixed, it is found that average density increases upon decreasing the value of Ω_D (detachment rate) (see Fig. 6).
- When system size N is increased, the amplitude of the shock increases and average density increases (see Fig. 8).
- Lane-changing rate Ω has almost no effect on density profiles in a two-lane TASEP coupled with Langmuir kinetics at a large attachment/detachment rate and/or a large system size.

Acknowledgements

R. Wang acknowledges the support of the ASIA:NZ Foundation Higher Education Exchange Program (2005), Massey University Research Fund (2005), and Massey University International Visitor Research Fund (2007). R. Jiang acknowledges the support of National Basic Research Program of China (2006CB 705500), the National Natural Science Foundation of China (NNSFC) under Key Project No. 10532060, Project Nos. 10404025, 10672160 and 70601026, and the CAS Special Foundation. We are grateful to Denise Newth for proofreading this manuscript.

References

1. B. Schmittmann, *Int. J. Mod. Phys. B* **4**(15), 2269 (1990).
2. J. Krug, *Phys. Rev. Lett.* **67**, 1882 (1991).
3. G. Tripathy and M. Barma, *Phys. Rev. Lett.* **78**, 3039 (1997)
4. K.T. Leung and J.S. Wang, *Int. J. Mod. Phys. C* **10**(5), 853 (1999).
5. R.A. Monetti and E.V. Albano, *Int. J. Mod. Phys. B* **16**(27), 4165 (2002).
6. H.K. Lee and Y. Okabe, *Int. J. Mod. Phys. c* **17**(2), 157 (2006).
7. B. Derrida, *Phys. Rep.* **301**, 65 (1998).
8. G.M. Schütz, in *Phase Transitions and Critical Phenomena*, Vol. 19, edited by C. Domb and J.L. Lebowitz (Academic Press, San Diego, 2001).
9. B. Widom, J.L. Viovy and A.D. Defontaines, *J. Physique I* **1**, 1759 (1991).
10. G.M. Schütz, *Int. J. Mod. Phys. B* **11**(1), 197 (1997).

11. L.B. Shaw, R.K.P. Zia and K.H. Lee, *Phys. Rev. E* **68**, 021910 (2003). L.B. Shaw, A.B. Kolomeisky and K.H. Lee, *J. Phys. A* **37**, 2105 (2004).
12. T. Chou, *Biophys. J.* **85**, 755 (2003).
13. S. Klumpp and R. Lipowsky, *J. Stat. Phys.* **113**, 233 (2003).
14. R. Jiang, Y.-M. Yuan and Q.-S. Wu, *Int. J. Mod. Phys. B* **19**(18), 2989 (2005).
15. G.A. Klein, K. Kruse, G. Cuniberti and F. Jülicher, *Phys. Rev. Lett.* **94**, 108102 (2005).
16. D.W. Huang, *Int. J. Mod. Phys. C* **13**(6), 739 (2002).
17. J.T. MacDonald, J.H. Gibbs and A.C. Pipkin, *Biopolymers* **6**, 1 (1968).
18. K. Kruse and K. Sekimoto, *Phys. Rev. E* **66**, 031904 (2002).
19. R. Lipowsky, S. Klumpp and T. Nieuwenhuizen, *Phys. Rev. Lett.* **87**, 108101 (2001). S. Klumpp and R. Lipowsky, *J. Stat. Phys.* **113**, 233 (2003).
20. A. Parmeggiani, T. Franosch and E. Frey, *Phys. Rev. Lett.* **90**, 086601 (2003), *Phys. Rev. E* **70**, 046101 (2004).
21. K. Nishinari, Y. Okada, A. Schadschneider and D. Chowdhury, *Phys. Rev. Lett.* **95**, 118101 (2005).
22. D. Chowdhury, A. Schadschneider and K. Nishinari, *Phys. Life Rev.* **2**, 318 (2005).
23. R.D. Astumian, *Science* **276**, 917 (1997).
24. J. Howard, *Mechanism of Motor Proteins and the Cytoskeleton* (Sunderland, Massachusetts: Sinauer Associates), (2001).
25. E. Pronina and A.B. Kolomeisky, *J. Phys. A* **37**, 9907 (2004).
26. E. Pronina and A.B. Kolomeisky, *Physica A* **372**, 12 (2006).
27. T. Mitsudo and H. Hayakawa, *J. Phys. A* **38**, 3087 (2005).
28. T. Reichenbach, T. Franosch and E. Frey, *Phys. Rev. Lett.* **97**, 050603 (2006).
29. R. Jiang, R. Wang and Q.S. Wu, *Physica A* **375** (1), 247 (2007).
30. A. Alberts et al., *The Molecular Biology of the Cell* (Garland, New York, 1994).
31. Y. Okada and N. Hirokawa, *Science* **283**, 1152 (1999).
32. J.C. Liao, Y.J. Yeong, D.E. Kim, S.S. Patel and G. Oster, *J. Mol. Biol.* **350**, 452 (2005).
33. L. Debnath, *Nonliear Partial Differential Equations for Sciences and Engineers* (Birkhäuser, Boston, 1997).
34. M.J. Lighthill and G.B. Whitham, *Proc. Roy. Soc. A* **229**, 281 (1955).
35. M.R. Evans, R. Juhász and L. Santen, *Phys. Rev. E* **68**, 026117 (2003)
36. I.T. Georgiev, B. Schmittmann and R.K.P. Zia, *Phys. Rev. Lett.* **94**, 115701 (2005).
37. St.M. Block, L.S.B. Goldstein and B.J. Schnapp, *Nature*, **348**, 348 (1990).